All-order results for the one-loop QED correction to the hyperfine structure in light H-like atoms

V. A. Yerokhin,[1,2] A. N. Artemyev,[1] V. M. Shabaev,[1,3] and G. Plunien[4]
[1]*Department of Physics, St. Petersburg State University, Oulianovskaya 1, Petrodvorets, St. Petersburg 198504, Russia*
[2]*Center for Advanced Studies, St. Petersburg State Polytechnical University, Polytekhnicheskaya 29, St. Petersburg 195251, Russia*
[3]*Max-Planck-Institut für Physik Komplexer Systeme, Nöthnitzer Strasse 38, D-01187 Dresden, Germany*
[4]*Institut für Theoretische Physik, TU Dresden, Mommsenstrasse 13, D-01062 Dresden, Germany*
(Received 25 June 2005; published 16 November 2005)

A calculation of the one-loop self-energy and vacuum-polarization corrections to the hyperfine splitting of the $1s$ and $2s$ states in light H-like ions is carried out to all orders in the parameter $Z\alpha$. Using the known values for the $Z\alpha$-expansion coefficients, the numerical data obtained are extrapolated from $Z=5$ and higher to $Z=0$, 1, and 2, with the resulting accuracy being significantly better than in previous evaluations. Our calculation shifts the theoretical value of the normalized difference of the $1s$ and $2s$ hyperfine-structure intervals in $^3He^+$ by 0.056 kHz and improves its accuracy.

DOI: 10.1103/PhysRevA.72.052510 PACS number(s): 31.30.Jv, 32.10.Fn, 12.20.Ds

INTRODUCTION

Hyperfine splitting of the ground state in light H-like systems, such as hydrogen, deuterium, tritium, and the helium-3 ion, has long been known experimentally with extremely high precision. The present-day theory of the ground-state hyperfine structure (hfs) is still far behind the experiment, due to a relatively large contribution of the nuclear-structure effects, which cannot be accurately calculated at present. One of the possibilities to overcome this difficulty [1] is to study the normalized difference $\Delta_{21}=8\nu_{2s}-\nu_{1s}$, where ν_{1s} and ν_{2s} are the $1s$ and the $2s$ hfs intervals, respectively. A large class of corrections to ν_{1s} and ν_{2s} (among them, all lowest-order nuclear effects) are proportional to the nonrelativistic electron density at the position of the nucleus ($r=0$) and, therefore, do not contribute to the difference Δ_{21}. Consequently, the theoretical study of this difference can be performed up to a much higher accuracy than that of ν_{1s} and ν_{2s} separately.

The experimental value of the difference Δ_{21} is obtained by combining results of two independent measurements of ν_{1s} and ν_{2s} and is known less precisely than ν_{1s}. The best accuracy is reached for the helium-3 ion in a combination of two relatively old results [2,3],

$$\Delta_{21}(^3\mathrm{He}^+) = 1\,189.979(71)\ \mathrm{kHz}. \tag{1}$$

Recent progress was achieved in the measurement of ν_{2s} in hydrogen [4] and deuterium [5], which significantly improved the corresponding experimental values for the difference Δ_{21}.

The theory of hfs and, specifically, of the difference Δ_{21} in light H-like atoms has recently been examined in detail in Ref. [6]. It is demonstrated that one of the major uncertainties in the theoretical prediction of $\Delta_{21}(^3\mathrm{He}^+)$ stems from the one-loop self-energy correction. The self-energy correction is also responsible for a significant part of the theoretical uncertainty for the ground-state hyperfine splitting in muonium [7].

The goal of the present investigation is to improve the numerical accuracy of the one-loop QED correction for the $1s$ and $2s$ states in light H-like atoms. Our consideration will be carried out to all orders in the parameter $Z\alpha$ (Z is the nuclear charge number and α is the fine-structure constant). All-order calculations of the self-energy hfs correction in H-like ions have been previously performed by numerous authors [8–15]. Different evaluations are generally in good agreement (except for the first two calculations; see the discussion in Ref. [14]). For high- and middle-Z ions, results for this correction can be presently considered as well established at the level of the experimental interest. In the low-Z region, however, the experimental accuracy is much higher and technical problems encountered in all-order calculations are more demanding than for higher-Z ions. It would be clearly preferable to perform a direct all-order calculation for $Z=1$ and 2 with an accuracy significantly higher than the one presently obtained from the $Z\alpha$ expansion, as was done for the Lamb shift [16]. However, such a project has not been realized yet. Blundell *et al.* [12] obtained the higher-order (in $Z\alpha$) contribution to the $1s$ self-energy correction for $Z=1$ by extrapolating their numerical results for higher Z. Similar procedure was employed in the investigation by two of us [14] for the self-energy correction to the $1s$ and $2s$ hfs intervals for $Z=1$ and 2.

The vacuum-polarization hfs correction was evaluated to all orders in $Z\alpha$ in Refs. [8,17,18] (without the magnetic-loop Wichmann-Kroll correction) and in Refs. [13,19] (complete calculations). However, the above studies were mainly concerned with high- and middle-Z ions, so that little information was provided about the behavior of the Wichmann-Kroll part of the vacuum-polarization correction in the low-Z region.

In the present work, we perform a calculation of the one-loop self-energy and vacuum-polarization corrections to the $1s$ and $2s$ hfs intervals in H-like ions. The paper is organized as follows. In Sec. I we evaluate the self-energy correction by employing the additional-subtraction scheme [20] that improves the convergence properties of the resulting partial-wave expansion. In this way, we significantly increase the accuracy of the numerical results for $Z\geqslant 5$ as compared to the previous evaluations. The vacuum-polarization correction is evaluated in Sec. II. The higher-order one-loop QED con-

 ©2005 The American Physical Society

tribution is inferred from our all-order results in Sec. III by subtracting the known terms of the $Z\alpha$ expansion. Finally, we discuss the experimental consequences of our calculation.

Relativistic units ($\hbar=c=m=1$) are used throughout the paper.

I. SELF-ENERGY CORRECTION

In this section we describe the evaluation of the self-energy hfs correction without any expansion in $Z\alpha$. We start with general formulas for the self-energy correction in the presence of an additional perturbing potential δV. To the first order in δV, the self-energy correction is given by the sum of the *irreducible*, the *reducible*, and the *vertex* corrections [21],

$$\Delta E_{\rm SE} = \Delta E_{\rm ir} + \Delta E_{\rm red} + \Delta E_{\rm ver}. \tag{2}$$

The irreducible part arises through a perturbation of the wave function,

$$\Delta E_{\rm ir} = \langle \delta a | \gamma^0 \widetilde{\Sigma}(\varepsilon_a) | a \rangle + \langle a | \gamma^0 \widetilde{\Sigma}(\varepsilon_a) | \delta a \rangle, \tag{3}$$

where $\widetilde{\Sigma}=\Sigma-\delta m$, δm is the one-loop mass counterterm, Σ is the one-loop self-energy function,

$$\Sigma(\varepsilon,\boldsymbol{x}_1,\boldsymbol{x}_2) = 2i\alpha\gamma^0 \int_{-\infty}^{\infty} d\omega\, \alpha_\mu \times G(\varepsilon-\omega,\boldsymbol{x}_1,\boldsymbol{x}_2)\alpha_\nu D^{\mu\nu}(\omega,\boldsymbol{x}_{12}), \tag{4}$$

G is the Dirac-Coulomb Green's function $G(\varepsilon)=[\varepsilon-\mathcal{H}(1-i0)]^{-1}$, $\mathcal{H}$ is the Dirac-Coulomb Hamiltonian, $D^{\mu\nu}$ is the photon propagator, $\alpha^\mu=(1,\boldsymbol{\alpha})$, and $\boldsymbol{x}_{12}=\boldsymbol{x}_1-\boldsymbol{x}_2$. The perturbed wave function is given by

$$|\delta a\rangle = \sum_n^{\varepsilon_n\neq\varepsilon_a} \frac{|n\rangle\langle n|\delta V|a\rangle}{\varepsilon_a-\varepsilon_n}. \tag{5}$$

The reducible part can be considered as a correction due to the first-order perturbation of the binding energy,

$$\Delta E_{\rm red} = \delta\varepsilon_a \langle a|\gamma^0 \left.\frac{\partial}{\partial\varepsilon}\widetilde{\Sigma}(\varepsilon)\right|_{\varepsilon=\varepsilon_a} |a\rangle, \tag{6}$$

where $\delta\varepsilon_a=\langle a|\delta V|a\rangle$. The vertex part is given by

$$\Delta E_{\rm ver} = \frac{i}{2\pi}\int_{-\infty}^{\infty} d\omega \times \sum_{n_1 n_2} \frac{\langle n_1|\delta V|n_2\rangle\langle a n_2|I(\omega)|n_1 a\rangle}{[\varepsilon_a-\omega-\varepsilon_{n_1}(1-i0)][\varepsilon_a-\omega-\varepsilon_{n_2}(1-i0)]}, \tag{7}$$

where $I(\omega)=e^2\alpha_\mu\alpha_\nu D^{\mu\nu}(\omega)$.

The self-energy correction to hfs is given by the above formulas, in which we should assume the perturbing potential to have the form of the Fermi-Breit interaction (the nuclear magnetic moment is denoted by $\boldsymbol{\mu}$),

$$\delta V \to V_{\rm hfs}(\boldsymbol{r}) = \frac{|e|}{4\pi}\frac{\boldsymbol{\alpha}\cdot(\boldsymbol{\mu}\times\boldsymbol{r})}{r^3}, \tag{8}$$

and the initial-state wave function $|a\rangle$ to be the wave function of the coupled system (electron+nucleus),

$$|a\rangle \to |FM_F Ij\rangle = \sum_{M_I m_a} C^{FM_F}_{IM_I j_a m_a} |IM_I\rangle |j_a m_a\rangle, \tag{9}$$

where $|IM_I\rangle$ denotes the nuclear wave function, $|j_a m_a\rangle$ is the electron wave function, F is the total momentum of the atom, and M_F is its projection. Radial integrations over the nuclear coordinates can easily be performed already in the general expressions. One can show that formulas (3)–(7) yield corrections to the hfs if we employ the perturbing interaction in the form

$$\delta V(\boldsymbol{r}) = \frac{E_F}{4/3(Z\alpha)^3}\frac{(\boldsymbol{r}\times\boldsymbol{\alpha})_z}{r^3}, \tag{10}$$

where E_F is the nonrelativistic Fermi energy, and consider the initial-state wave function to be the electron wave function with the moment projection $m_a=1/2$,

$$|a\rangle = |j_a\, 1/2\rangle. \tag{11}$$

A. Irreducible part

As follows from Eq. (3), evaluation of the irreducible part of the self-energy hfs correction implies a calculation of a nondiagonal matrix element of the self-energy function and, therefore, is very similar to the evaluation of the first-order self-energy correction to the Lamb shift. Since our present approach to this problem is somewhat different from the standard potential-expansion method, we now give a short description of the scheme used for the evaluation of a self-energy matrix element.

Ultraviolet divergencies in the self-energy function (4) are traditionally isolated by separating the first two terms in the expansion of the bound-electron propagator G in terms of the binding potential V,

$$G(E,\boldsymbol{x}_1,\boldsymbol{x}_2) = G^{(0)}(E,\boldsymbol{x}_1,\boldsymbol{x}_2) + G^{(1)}(E,\boldsymbol{x}_1,\boldsymbol{x}_2) + G^{(2+)}(E,\boldsymbol{x}_1,\boldsymbol{x}_2), \tag{12}$$

where $G^{(0)}=[\omega-\mathcal{H}_0(1-i0)]^{-1}$ is the free Dirac Green's function, $G^{(1)}$ is the first-order expansion term

$$G^{(1)}(E,\boldsymbol{x}_1,\boldsymbol{x}_2) = \int d\boldsymbol{z}\, G^{(0)}(E,\boldsymbol{x}_1,z)V(z)G^{(0)}(E,z,\boldsymbol{x}_2), \tag{13}$$

and $G^{(2+)}$ is the remainder. Representing G in the form (12) leads to splitting the matrix element of the self-energy function into zero-potential, one-potential, and many-potential parts (see Refs. [22–24] for details),

$$\langle a|\gamma^0\widetilde{\Sigma}(\varepsilon_a)|a\rangle = \Delta E_{\rm zero} + \Delta E_{\rm one} + \Delta E_{\rm many}, \tag{14}$$

with the mass-counterterm part naturally ascribed to the zero-potential term.

Modifications of the standard potential-expansion approach introduced in our previous investigation [20] concern the many-potential term, which is given by

$$\Delta E_{\rm many} = 2i\alpha \int_{C_{LH}} d\omega \int d\boldsymbol{x}_1 d\boldsymbol{x}_2 D^{\mu\nu}(\omega,\boldsymbol{x}_{12}) \psi_a^\dagger(\boldsymbol{x}_1)\alpha_\mu \times G^{(2+)}(\varepsilon_a-\omega,\boldsymbol{x}_1,\boldsymbol{x}_2)\alpha_\nu \psi_a(\boldsymbol{x}_2). \tag{15}$$

The integration contour C_{LH} consists of two parts, the low-energy (C_L) and the high-energy (C_H) one. The low-energy part extends from ε_0-i0 to $-i0$ on the lower bank of the branch cut of the photon propagator and from $i0$ to ε_0+i0 on the upper bank of the cut. In order to avoid the appearance of poles of the electron propagator near the integration contour, each part of C_L is bent into the complex plane if the calculation is performed for an excited state. The high-energy part of the contour is $C_H=(\varepsilon_0-i\infty,\varepsilon_0-i0]+[\varepsilon_0+i0,\varepsilon_0+i\infty)$. The parameter ε_0 of the contour is chosen arbitrarily from the interval $\varepsilon_0\in(\varepsilon_a-\varepsilon_{1s},1+\varepsilon_a)$, where ε_{1s} is the ground-state energy.

The function $G^{(2+)}=G-G^{(0)}-G^{(1)}$ that enters Eq. (15) is not known in its closed form at present and, consequently, evaluation of the many-potential term has to be performed by expanding G (and, therefore, $G^{(2+)}$) into eigenfunctions of the Dirac angular momentum with the eigenvalue κ. This expansion will be referred to as the partial-wave expansion in the following. Its convergence properties are of crucial importance for the numerical evaluation of the self-energy correction.

In our previous investigation [20], it was demonstrated that the convergence rate of the partial-wave expansion could be significantly enhanced by separating from $G^{(2+)}$ a part that is calculated in a closed form. It was found that in the region $\boldsymbol{x}_1\approx\boldsymbol{x}_2$ the function $G^{(2+)}$ could be approximated by a simpler function $G_a^{(2+)}$ of the form

$$G_a^{(2+)}(E,\boldsymbol{x}_1,\boldsymbol{x}_2) = G^{(0)}(E+\Omega,\boldsymbol{x}_1,\boldsymbol{x}_2) - G^{(0)}(E,\boldsymbol{x}_1,\boldsymbol{x}_2) - \Omega\frac{\partial}{\partial E}G^{(0)}(E,\boldsymbol{x}_1,\boldsymbol{x}_2), \tag{16}$$

where

$$\Omega = \frac{2Z\alpha}{x_1+x_2}. \tag{17}$$

The above approximation can be obtained from the (exact) potential expansion of $G^{(2+)}$,

$$G^{(2+)} = G^{(0)}VG^{(0)}VG^{(0)} + G^{(0)}VG^{(0)}VG^{(0)}VG^{(0)} + \cdots, \tag{18}$$

by neglecting the commutators $[V,G^{(0)}]$ to all orders [or, in other words, by expanding all binding potentials $V(\boldsymbol{x})$ around the point $\boldsymbol{x}=\boldsymbol{x}_1$ or $\boldsymbol{x}=\boldsymbol{x}_2$ and keeping only the first terms; details can be found in Ref. [20]]. After this approximation is made, the series acquires the form of the Taylor expansion and can be summed up in a closed form.

It should be noted that the idea of commuting the potential V outside was first proposed by Mohr [25], who proved that this procedure does not influence the asymptotic ultraviolet behavior of the one-potential term (we recall that ultraviolet divergences originate from the region $\boldsymbol{x}_1\approx\boldsymbol{x}_2$ in configuration space). Later it was also demonstrated [26,27] that all ultraviolet divergences in the one-loop self-energy correction could be identified by isolating several terms of the power-series expansion of the potential V and the reference-state wave functions ψ_a around the point $\boldsymbol{x}_1=\boldsymbol{x}_2$. The distinct features of the present approach compared to the previous studies are that this expansion is carried out to all orders in the potential V and that the result is written in a closed form.

The function $G_a^{(2+)}$ is expressed in terms of the free Green's function and can be easily evaluated. We thus write $\Delta E_{\rm many}$ as a sum of two terms,

$$\Delta E_{\rm many} = \Delta E_{\rm many}^{\rm sub} + \Delta E_{\rm many}^{\rm remd}. \tag{19}$$

The subtraction term $\Delta E_{\rm many}^{\rm sub}$ is obtained from the high-energy part of Eq. (15) by the substitution $G^{(2+)}\to G_a^{(2+)}$. The second term $\Delta E_{\rm many}^{\rm remd}$ is the remainder. The subtraction term is evaluated numerically in its closed form (i.e., without any partial-wave expansion), whereas the remainder yields a rapidly converging partial-wave expansion. Further details of the numerical procedure for the evaluation of the one-loop self-energy correction can be found in Ref. [20].

B. Reducible part

The reducible part is defined by Eq. (6). Using the definition of the self-energy function and employing the contour C_{LH} for the integration over ω, we write the expression in the form

$$\Delta E_{\rm red} = 2i\alpha\delta\varepsilon_a \int_{C_{LH}} d\omega \int d\boldsymbol{x}_1 d\boldsymbol{x}_2 D^{\mu\nu}(\omega,\boldsymbol{x}_{12}) \times \psi_a^\dagger(\boldsymbol{x}_1)\alpha_\mu \left.\frac{\partial}{\partial\varepsilon}G(\varepsilon-\omega,\boldsymbol{x}_1,\boldsymbol{x}_2)\right|_{\varepsilon=\varepsilon_a} \alpha_\nu\psi_a(\boldsymbol{x}_2). \tag{20}$$

Ultraviolet (UV) and infrared (IR) divergences present in this expression can be conveniently isolated by separating the Green's function G into three parts,

$$G(E) = G^{(0)}(E) + G^{(a)}(E) + [G(E) - G^{(0)}(E) - G^{(a)}(E)], \tag{21}$$

where $G^{(a)}$ incorporates the part of the spectral decomposition of the bound-electron propagator with $\varepsilon_n=\varepsilon_a$,

$$G^{(a)}(E,\boldsymbol{x}_1,\boldsymbol{x}_2) = \sum_{\mu_a} \frac{\psi_a(\boldsymbol{x}_1)\psi_a^\dagger(\boldsymbol{x}_2)}{E-\varepsilon_a(1-i0)}, \tag{22}$$

and μ_a denotes the momentum projection of the states ψ_a in this expression. The terms on the right-hand side of Eq. (21) substituted in Eq. (20) give rise to the splitting of $\Delta E_{\rm red}$, correspondingly, into three parts:

$$\Delta E_{\rm red} = \Delta E_{\rm red}^{(0)} + \Delta E_{\rm red}^{(a)} + \Delta E_{\rm red}^{\rm many}. \tag{23}$$

In this sum, the term $\Delta E_{\rm red}^{(0)}$ contains all UV divergences. It is calculated in momentum space in a way similar to that for

TABLE I. Individual contributions to the self-energy hfs correction for $Z=10$, in units of the function $D_n^{\rm SE}$ defined by Eq. (30).

	$\Delta E_{\rm ir}$	$\Delta E_{\rm red}^{(0)}+\Delta E_{\rm ver}^{(0)}$	$\Delta E_{\rm red}^{(a)}+\Delta E_{\rm ver}^{(a)}$	$\Delta E_{\rm red}^{\rm many}$	$\Delta E_{\rm ver}^{\rm many}$	Total
$1s$	−0.263902	1.896440	−0.002385	−1.607827	−0.185180	−0.162853(1)
$2s$	−0.223649	3.433554	0.176267	−1.878883	−1.649848	−0.142559(3)

the zero-potential part of the first-order self-energy correction. UV-divergent terms are covariantly isolated; they disappear when combined with the free-propagator contribution in the vertex part. The term $\Delta E_{\rm red}^{(a)}$ contains all IR divergences present in the reducible part. (IR divergences of this type are sometimes also termed as the *reference-state* singularities.) These divergences are regularized by employing the photon propagator with a finite photon mass μ. The limit $\mu\to 0$ can be taken when $\Delta E_{\rm red}^{(a)}$ is combined with the corresponding contribution from the vertex part.

The term $\Delta E_{\rm red}^{\rm many}$ is finite. Contributions of such type are frequently encountered in all-order QED calculations. Usually, they are evaluated in coordinate space after expanding into an infinite partial-wave series. In the present investigation, we modify the standard scheme in order to achieve a better convergence of the partial-wave expansion, analogously to that for the irreducible part. We thus separate $\Delta E_{\rm red}^{\rm many}$ into two parts,

$$\Delta E_{\rm red}^{\rm many} = \Delta E_{\rm red}^{\rm sub} + \Delta E_{\rm red}^{\rm remd}. \tag{24}$$

The remainder term $\Delta E_{\rm red}^{\rm remd}$ is obtained from $\Delta E_{\rm red}^{\rm many}$ by replacing the standard subtraction $[G(E)-G^{(0)}(E)-G^{(a)}(E)]$ by $[G(E)-G^{(0)}(E+\Omega)-G^{(a)}(E)]$ in the high-energy part of the expression. The remaining difference $[G^{(0)}(E+\Omega)-G^{(0)}(E)]$ gives rise to the subtraction term $\Delta E_{\rm red}^{\rm sub}$. More explicitly, the subtraction term is written as

$$\Delta E_{\rm red}^{\rm sub} = 2i\alpha\delta\varepsilon_a \int_{C_H} d\omega \int d\boldsymbol{x}_1 d\boldsymbol{x}_2 D^{\mu\nu}(\omega,\boldsymbol{x}_{12}) \times \psi_a^\dagger(\boldsymbol{x}_1)\alpha_\mu \frac{\partial}{\partial\varepsilon}[G^{(0)}(\varepsilon-\omega+\Omega,\boldsymbol{x}_1,\boldsymbol{x}_2) - G^{(0)}(\varepsilon-\omega,\boldsymbol{x}_1,\boldsymbol{x}_2)]\Big|_{\varepsilon=\varepsilon_a} \alpha_\nu\psi_a(\boldsymbol{x}_2), \tag{25}$$

where Ω is given by Eq. (17). This expression is calculated in its closed form in coordinate space. The calculational formulas are immediately obtained from the corresponding expressions for the subtraction term for the first-order self-energy correction [20]. The remainder term is calculated by a partial-wave expansion. Due to the additional subtraction in the high-energy part, the convergence properties of this partial-wave expansion are much better than in the standard approach.

C. Vertex part

Rewriting expression (7) for the vertex part of the self-energy hfs correction in terms of the bound-electron propagators, we obtain

$$\Delta E_{\rm ver} = 2i\alpha \int_{C_{LH}} d\omega \int d\boldsymbol{x}_1 d\boldsymbol{x}_2 d\boldsymbol{x}_3 \psi_a^\dagger(\boldsymbol{x}_1)\alpha_\mu \times G(\varepsilon_a-\omega,\boldsymbol{x}_1,\boldsymbol{x}_2)\delta V(\boldsymbol{x}_2) G(\varepsilon_a-\omega,\boldsymbol{x}_2,\boldsymbol{x}_3) \times \alpha_\nu\psi_a(\boldsymbol{x}_3) D^{\mu\nu}(\omega,\boldsymbol{x}_{13}). \tag{26}$$

UV and IR divergences present in this expression can be conveniently isolated by the following separation:

$$G\delta VG = G^{(0)}\delta VG^{(0)} + G^{(a)}\delta VG^{(a)} + (G\delta VG - G^{(0)}\delta VG^{(0)} - G^{(a)}\delta VG^{(a)}). \tag{27}$$

This separation, being substituted into Eq. (26), gives rise to the following three parts of $\Delta E_{\rm ver}$:

$$\Delta E_{\rm ver} = \Delta E_{\rm ver}^{(0)} + \Delta E_{\rm ver}^{(a)} + \Delta E_{\rm ver}^{\rm many}. \tag{28}$$

Only the first term in this sum is UV divergent. UV divergences in $\Delta E_{\rm ver}^{(0)}$ are covariantly isolated by employing a momentum-space representation; they disappear when combined with the corresponding contribution from the reducible part (see, e.g., Ref. [10]). The second term $\Delta E_{\rm ver}^{(a)}$ is IR divergent. In order to retain its finite part, we consider it together with the corresponding contribution from the reducible part,

$$\Delta E_{\rm ver}^{(a)} + \Delta E_{\rm red}^{(a)} = \frac{i}{2\pi}\int_{C_{LH}} d\omega \frac{1}{(\omega-i0)^2} \times \left(\sum_{\mu_{a'}\mu_{a''}} \langle a'|\delta V|a''\rangle\langle aa''|I(\omega)|a'a\rangle - \sum_{\mu_{a'}} \langle a|\delta V|a\rangle\langle aa'|I(\omega)|a'a\rangle \right), \tag{29}$$

where a' and a'' denote the intermediate states with $\varepsilon_n=\varepsilon_a$ and with the momentum projection $\mu_{a'}$ and $\mu_{a''}$, respectively. The integration over ω can be carried out analytically, which leads to an explicitly finite result. Sometimes it is more convenient to calculate this contribution directly according to Eq. (29) (as long as the contour C_{LH} is employed for the integration over ω, this expression is suitable for the numerical evaluation).

The third term $\Delta E_{\rm ver}^{\rm many}$ does not contain any divergences and is calculated in coordinate space after expanding into a partial-wave series. We note that an additional subtraction, similar to the one introduced for the reducible part, does not improve the convergence properties of the partial-wave expansion in this case. This is due to the fact that a significant contribution to the partial-wave expansion terms originates from the first-order commutator $[V,G^{(0)}]$. In order to achieve a significant improvement, one needs to separate the complete contribution of the vertex with one magnetic and one Coulomb interaction. Such contribution was evaluated in a

TABLE II. The self-energy hfs correction for the $n=1$ and 2 states of light H-like ions.

Z	$D_1^{\rm SE}(Z\alpha)$	$D_2^{\rm SE}(Z\alpha)$
5	0.174 026 (2)	0.181 940 (2)
6	0.106 815 (2)	0.117 124 (2)
7	0.039 476 (2)	0.052 265 (2)
8	−0.027 933(1)	−0.012 626(2)
9	−0.095 379(1)	−0.077 559(3)
10	−0.162 853(1)	−0.142 559(3)
12	−0.297 905(1)	−0.272 913(1)
15	−0.501 056(1)	−0.470 078(1)
20	−0.843 572(1)	−0.807 153(1)
25	−1.196 242(2)	−1.162 717(2)
30	−1.566 491(3)	−1.547 535(2)

closed form for the self-energy correction to the g factor [28,29] using the explicit form of the interaction with the constant magnetic field. In the case of the self-energy hfs correction, we are presently unable to obtain a closed representation for this term. Nevertheless, the partial-wave expansion for $\Delta E_{\rm ver}^{\rm many}$ is converging significantly faster than that for $\Delta E_{\rm ir}^{\rm many}$ and $\Delta E_{\rm red}^{\rm many}$, so that the enhanced convergence achieved for the irreducible and reducible parts results finally in a significant improvement of the total accuracy of the calculation.

D. Numerical results

The one-loop radiative corrections to the hyperfine splitting are conveniently represented in terms of the dimensionless function D_n defined as

$$\Delta E = \frac{E_F}{n^3}\frac{\alpha}{\pi}D_n(Z\alpha), \tag{30}$$

where n is the principal quantum number. The self-energy and vacuum-polarization parts of the function $D_n(Z\alpha)$ will be in the following referred to as $D_n^{\rm SE}(Z\alpha)$ and $D_n^{\rm VP}(Z\alpha)$, respectively.

The numerical results for individual contributions to the self-energy hfs correction for the $1s$ and $2s$ states and $Z=10$ are presented in Table I. The calculation was performed for the point nuclear model and in the Feynman gauge. In Table II we list the final results for the self-energy hfs correction for H-like ions with Z varying from 5 to 30. A comparison of the results of different theoretical evaluations for this correction in the low-Z region is given in Table III.

As can be seen from Table III, the present calculation improves the numerical accuracy of the self-energy hfs correction by about an order of magnitude for the $1s$ state and even more for the $2s$ state, as compared to our previous calculation [14]. This progress is due to the additional subtraction scheme employed in the present work for the evaluation of the irreducible and reducible parts of the correction. In order to illustrate the improvement in the convergence properties of the partial-wave expansion introduced by this scheme, in Figs. 1 and 2 we plot the dependence of the absolute value of the individual terms of the partial-wave series on the expansion parameter $|\kappa|$ within the standard potential-expansion approach and within the present subtraction scheme. (The parameter κ is the Dirac angular-momentum eigenvalue of one of the electron propagators in the vertex function.) Figures 1 and 2 represent this comparison for the irreducible and reducible parts, respectively.

As a result of the improvement achieved, we were able to eliminate completely the uncertainty arising from termination of the partial-wave expansion in the irreducible and reducible parts. Still, there remains the partial-wave expansion of the many-potential vertex term $\Delta E_{\rm ver}^{\rm many}$, which has to be terminated and properly extrapolated to infinity. (In actual calculations the summation was terminated at $|\kappa|=40$.) The error due to this extrapolation yields one of the main uncertainties of our numerical evaluation (the other source of uncertainty is the stability of numerical integrations.) Fortunately, the partial-wave expansion of $\Delta E_{\rm ver}^{\rm many}$ is monotonic and relatively well converging (not worse than $1/|\kappa|^3$ for all $Z\geqslant 5$), and so the uncalculated tail of the expansion can be estimated reasonably well.

II. VACUUM-POLARIZATION CORRECTION

The vacuum-polarization hfs correction can be conveniently split into two parts, the so-called *electric-* and *magnetic-loop* contributions. The electric-loop part originates from the diagrams with the hfs interaction attached to the external electron line, whereas the magnetic-loop one comes from the diagram with the hfs interaction attached to the vacuum-polarization loop. These contributions are also traditionally separated into the Uehling and Wichmann-Kroll

TABLE III. Comparison of the results of different calculations of the self-energy hfs correction for the $1s$ and $2s$ states in light H-like ions, in terms of $D_n^{\rm SE}(Z\alpha)$.

	$Z=5$	$Z=10$	$Z=20$	Reference
$1s$	0.174 026(2)	−0.162 853(1)	−0.843 572(1)	
	0.174 028(20)	−0.162 860(20)	−0.843 588(15)	[14]
	0.174 05(1)	−0.162 83(1)	−0.843 56(1)	[12]
	0.174 1(1)	−0.162 8(1)		[13]
$2s$	0.181 940(2)	−0.142 559(3)	−0.807 153(1)	
	0.181 96(10)	−0.142 51(10)	−0.807 16(6)	[14]

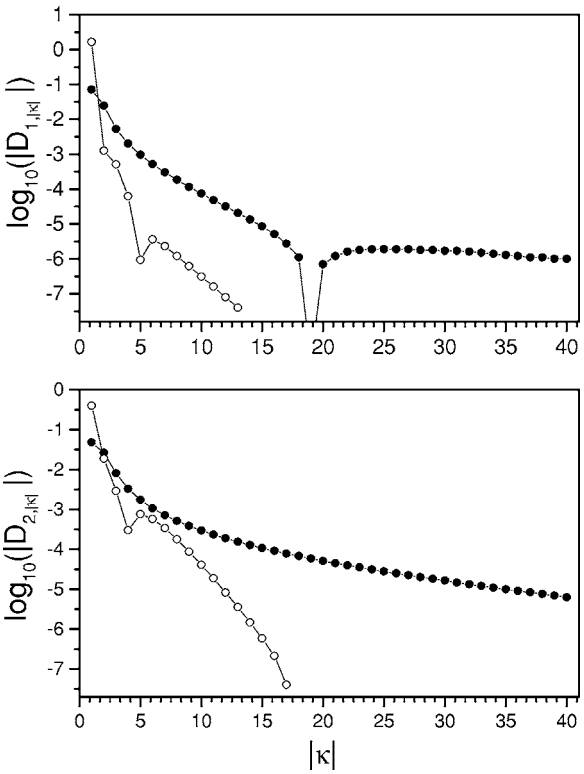

FIG. 1. The absolute magnitude of the individual terms of the partial-wave expansion for the irreducible part of the self-energy hfs correction ($Z=5$) for the $1s$ state (the upper graph) and for the $2s$ state (the lower graph), within the standard potential-expansion scheme (filled dots) and with the additional subtraction employed in the present work (open dots). Plotted are the contributions to the function $D_n(Z\alpha)$ as a function of the absolute value of the relativistic angular momentum parameter κ. A discontinuity of the curve on the upper graph around $|\kappa|=19$ is due to the change of the sign of the contributions to $D_1(Z\alpha)$.

(WK) parts. The WK part is suppressed by a factor of $(Z\alpha)^2$ as compared to the Uehling contribution and can often be regarded as a small correction for low-Z ions.

The $Z\alpha$ expansion of the one-loop vacuum-polarization hfs correction reads

$$D_n^{\rm VP}(Z\alpha) = (Z\alpha)b_{10} + (Z\alpha)^2(Lb_{21} + b_{20}) + (Z\alpha)^3[Lb_{31} + F_n^{\rm VP}(Z\alpha)], \tag{31}$$

where the function $D_n^{\rm VP}$ is related to the energy shift as defined by Eq. (30), $L=\ln[(Z\alpha)^{-2}]$, and the function $F_n^{\rm VP}$ incorporates all higher-order terms, $F_n^{\rm VP}(Z\alpha)=b_{30}+Z\alpha(\cdots)$. The first expansion coefficients up to b_{31} stem from the Uehling part of the vacuum-polarization correction; they are given by (see Refs. [30–32] and references therein)

$$b_{10}(ns) = \frac{3\pi}{4}, \tag{32}$$

$$b_{21}(ns) = \frac{8}{30}, \tag{33}$$

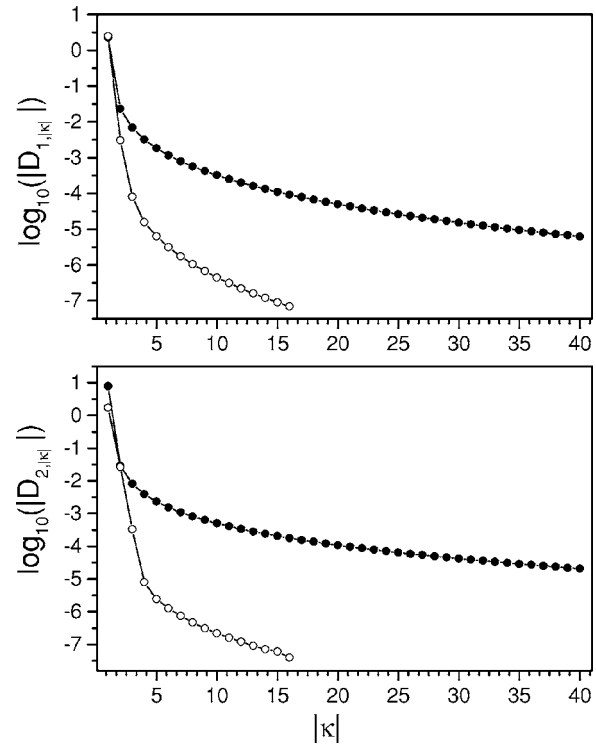

FIG. 2. The same as in Fig. 1, but for the reducible part of the self-energy hfs correction.

$$b_{20}(1s) = \frac{34}{225} - \frac{8}{15}\ln 2, \tag{34}$$

$$b_{20}(2s) = -\frac{247}{450}, \tag{35}$$

$$b_{31}(ns) = \frac{13\pi}{48}. \tag{36}$$

Higher-order coefficients starting with b_{30} arise from both the Uehling and WK contributions; only their Uehling part is presently known.

The Uehling part of the one-loop vacuum-polarization hfs correction can easily be calculated numerically; some results can be found, e.g., in Refs. [13,19]. In the case of the point nucleus, this contribution was evaluated also analytically [6,33]. For completeness, we recalculate it in the present work. The corresponding contributions to the higher-order remainder $F_n^{\rm VP}(Z\alpha)$ for the point nuclear model are listed in the first and second columns of Table IV for the $1s$ and $2s$ states, respectively. The results presented are in agreement with the previous calculations of this correction.

The WK part of the vacuum-polarization hfs correction is more difficult to calculate. This refers especially to the magnetic-loop WK contribution. As outlined in Ref. [19], this correction is divergent in the point-dipole approximation for the nuclear magnetization distribution. A finite result for this correction is obtained if an extended nuclear magnetization distribution is employed. It should be also taken into account that the magnetic-loop WK interaction contributes to

TABLE IV. Individual contributions to $F_n^{\rm VP}(Z\alpha)$ for the $1s$ and $2s$ states of light H-like ions.

	Uehling		Electric-loop WK		Magnetic-loop WK	
Z	$1s$	$2s$	$1s$	$2s$	$1s$	$2s$
1	7.231	9.546	−0.117	−0.117		
2	7.337	9.651	−0.120	−0.119		
5	7.587	9.901	−0.128	−0.125		
10	7.947	10.282	−0.138	−0.133	−0.699(2)	−0.706(2)
			−0.139[a]		−0.697[a]	
12	8.092	10.441	−0.142	−0.136	−0.701(2)	−0.709(2)
14	8.240	10.609	−0.145	−0.138	−0.703(2)	−0.714(2)
16	8.394	10.788	−0.149	−0.141	−0.705(2)	−0.718(2)
18	8.556	10.978	−0.153	−0.145	−0.707(2)	−0.723(2)
			−0.154[a]		−0.706[a]	
20	8.725	11.182	−0.156	−0.148	−0.712(2)	−0.732(2)
22	8.904	11.401	−0.160	−0.151	−0.717(2)	−0.740(2)
24	9.093	11.635	−0.164	−0.155	−0.725(2)	−0.752(2)

[a]Reference [13].

the measured value of the nuclear magnetic moment [34]. In order to prevent double counting, the corresponding contribution should be subtracted from the magnetic-loop WK part of the vacuum-polarization hfs correction. Practical calculations [13,19] show that, after such a subtraction, the magnetic-loop WK correction depends weakly on details of the nuclear magnetization distribution and has a finite limit in the point-dipole approximation.

The results of our numerical evaluation of the electric- and magnetic-loop WK contributions for the $1s$ and $2s$ states of light H-like ions are listed in Table IV, in terms of the higher-order remainder $F_n^{\rm VP}(Z\alpha)$. The electric-loop WK correction was calculated for the point nuclear model by employing the analytical-approximation formulas for the WK potential from Ref. [35]. The relative accuracy of this approximation is considered by the authors to be not worse than 10^{-4} for all Z up to $Z\alpha=0.95$. As an independent test of the accuracy of this approximation in the low-Z region, we checked that it reproduces well the first two terms of the $Z\alpha$ expansion of the WK correction to the Lamb shift. The magnetic-loop WK correction was calculated for the point-dipole nuclear magnetization model by using a code developed in our previous investigation [19]. A comparison given in Table IV demonstrates good agreement of our numerical values with the $1s$ results of Ref. [13] for $Z=10$ and 18.

III. HIGHER-ORDER ONE-LOOP QED CORRECTION

One of the goals of our investigation is to improve the accuracy of the one-loop QED correction for $Z=1$ and 2, these being the most interesting cases from the experimental point of view. The present approach does not employ the $Z\alpha$ expansion and, therefore, our numerical results do not suffer from omission of the higher-order terms, as is the case with the perturbative $Z\alpha$-expansion approach. But on the other hand, technical problems do not presently allow us to perform a direct numerical evaluation for $Z=1$ and 2 with a sufficient accuracy. In the present work, we employ an indirect method used previously in Refs. [12,14]. By subtracting the known terms of the $Z\alpha$ expansion from the all-order results for higher values of Z, we identify the higher-order remainder and then extrapolate it to $Z=1$ and 2.

First we summarize the results obtained for the one-loop self-energy hfs correction within the perturbative $Z\alpha$-expansion approach. The corresponding $Z\alpha$ expansion reads

$$D_n^{\rm SE}(Z\alpha) = a_{00} + (Z\alpha)a_{10} + (Z\alpha)^2(L^2a_{22} + La_{21} + a_{20}) + (Z\alpha)^3[La_{31} + F_n^{\rm SE}(Z\alpha)], \tag{37}$$

where the function $D_n^{\rm SE}$ is related to the energy shift as defined by Eq. (30), $L=\ln[(Z\alpha)^{-2}]$, and $F_n^{\rm SE}$ is the remainder containing all higher-order terms, $F_n^{\rm SE}(Z\alpha)=a_{30}+Z\alpha(\cdots)$. The results presently available for the expansion coefficients are (see Refs. [32,36,37] and references therein for earlier studies)

$$a_{00}(ns) = \frac{1}{2}, \tag{38}$$

$$a_{10}(ns) = \left(\ln 2 - \frac{13}{4}\right)\pi, \tag{39}$$

$$a_{22}(ns) = -\frac{2}{3}, \tag{40}$$

$$a_{21}(1s) = -\frac{8}{3}\ln 2 + \frac{37}{72}, \tag{41}$$

$$a_{21}(2s) = a_{21}(1s) - \frac{8}{3}\ln 2 + \frac{7}{2}, \tag{42}$$

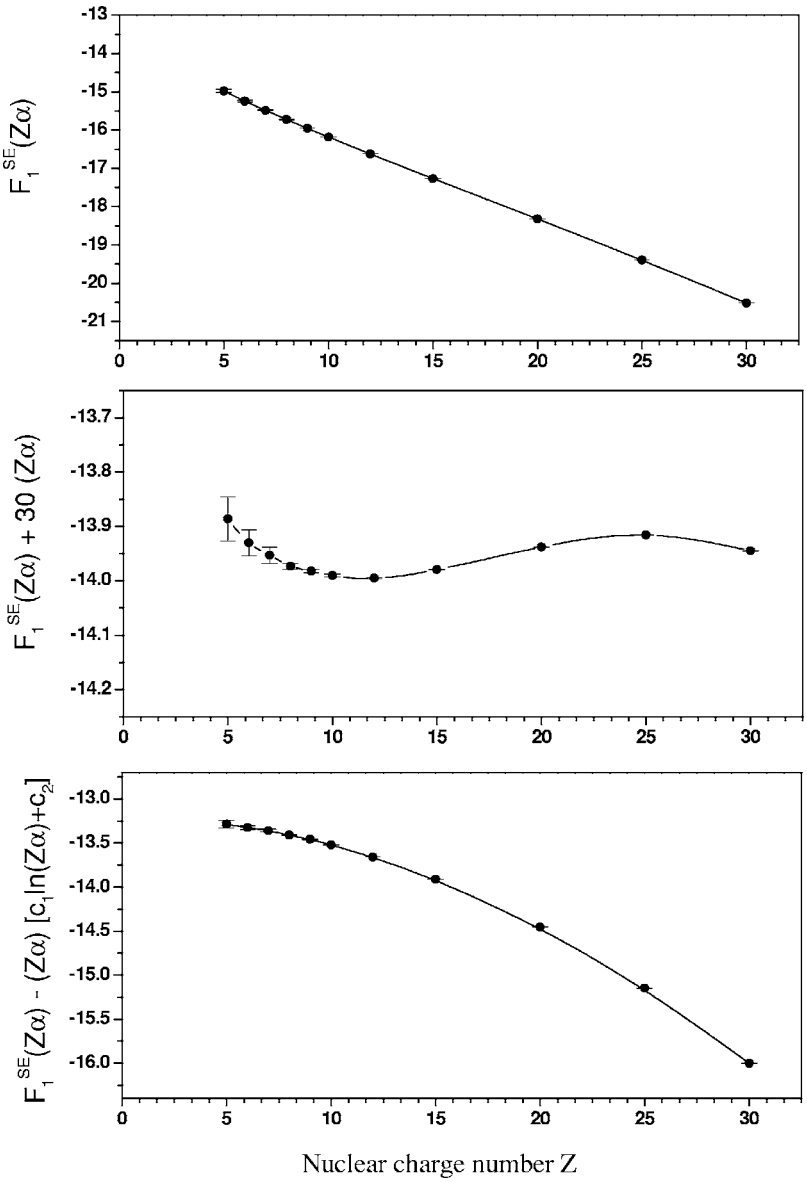

FIG. 3. The higher-order remainder of the $1s$ self-energy hfs correction F_1^{SE} as a function of the nuclear charge number (the upper graph); F_1^{SE} with its linear part (obtained by a global linear fit) subtracted (the middle graph); F_1^{SE} with its next-to-leading contribution (obtained by a least-squares fit) subtracted (the lower graph). The numerical values of the coefficients c_1 and c_2 are $c_1=14.83$ and $c_2=2.08$.

$$a_{20}(1s) = 17.122\,339\ldots, \tag{43}$$

$$a_{20}(2s) = a_{20}(1s) - 5.221\,233(3), \tag{44}$$

$$a_{31}(ns) = \left(\frac{5}{2}\ln 2 - \frac{191}{32}\right)\pi. \tag{45}$$

For the a_{30} term, there is a preliminary result [38] for the $1s$ state, $a_{30}(1s)=-15.9(1.6)$, and a partial result [6,39] for the difference Δ_{21}, $a_{30}(2s)-a_{30}(1s)=7.92$.

The higher-order self-energy remainder F_n^{SE} can be inferred from our all-order numerical data. The corresponding results for the function $F_1^{\mathrm{SE}}(Z\alpha)$ and the difference $F_{21}^{\mathrm{SE}}(Z\alpha) \equiv F_2^{\mathrm{SE}}(Z\alpha)-F_1^{\mathrm{SE}}(Z\alpha)$ are plotted on the upper graphs of Figs. 3 and 4, respectively. We note that both $F_1^{\mathrm{SE}}(Z\alpha)$ and $F_{21}^{\mathrm{SE}}(Z\alpha)$ have a rapidly varying structure in the low-Z region. In order to demonstrate this more clearly, we subtract their "linear" part (obtained by a global linear fit), with the corresponding plots presented on the middle graphs of Figs. 3 and 4. The behavior observed apparently indicates that logarithmic terms to order $\alpha(Z\alpha)^4E_F$ enter with large coefficients, which complicates extrapolation considerably.

Now we would like to extrapolate our results for the higher-order remainder to the lower values of Z, namely, $Z=0$, 1, and 2. For this purpose we employ a procedure similar to the one recently described in detail in Ref. [40]. The extrapolated value of a function at $Z=z_0$ is obtained in two steps. First we apply an (exact) linear fit to each two consecutive points from our data set and store the resulting value at $Z=z_0$ as a function of the average abscissa of the points involved in the fit. Then we perform a global parabolic least-squares fit to the set of data obtained and take the fitted value at $Z=z_0$ as a result.

We tested this procedure for variation of the logarithmic contribution to the next-to-leading order and found it rather stable. However, in order to take into account the presence of such contribution explicitly, we modify the procedure described above as follows. First, we approximate our numerical data by a function $f(Z)$ of the form

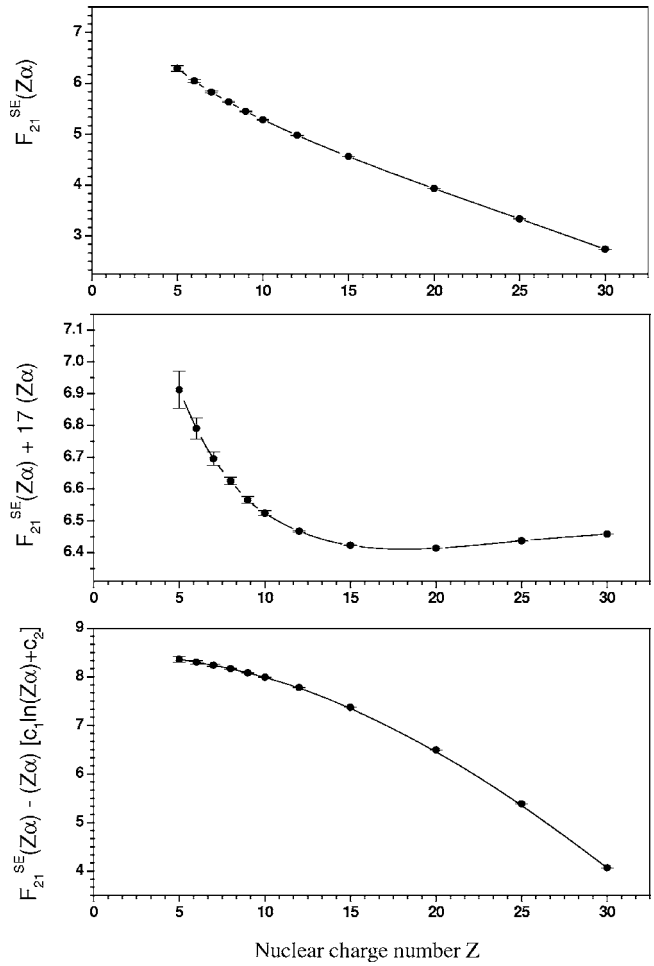

FIG. 4. The same as in Fig. 3 but for the difference $F_{21}^{\mathrm{SE}}=F_2^{\mathrm{SE}}-F_1^{\mathrm{SE}}$. The numerical values of the coefficients c_1 and c_2 are $c_1=28.26$ and $c_2=36.85$.

$$f(Z) = c_0 + (Z\alpha)[c_1 \ln(Z\alpha) + c_2 + (Z\alpha)c_3] \tag{46}$$

with free coefficients c_i, which are determined by a least-squares fit similar to the one described in Ref. [41]. Then we use the values obtained for c_1 and c_2 in order to define a modified higher-order remainder function as

$$\tilde{F}_n^{\mathrm{SE}}(Z\alpha) = F_n^{\mathrm{SE}}(Z\alpha) - (Z\alpha)[c_1 \ln(Z\alpha) + c_2]. \tag{47}$$

The numerical results for this function are plotted on the lower graphs of Figs. 3 and 4. The function $\tilde{F}_n^{\mathrm{SE}}$ is much flatter in the low-Z region than F_n^{SE} and, therefore, is more suitable for the extrapolation. We obtain our final results extrapolating the function $\tilde{F}_n^{\mathrm{SE}}$ by means of the procedure described above. The numerical values of the higher-order self-energy remainder obtained in this way are given in the first line of Table V. In the next three lines of the table, we present the results of the previous evaluations [12,14,38]. The numerical values obtained for the function F_{21}^{SE} in this work fall slightly outside the error bars ascribed to our previous results [14], as a consequence of the logarithmic contribution to the next-to-leading order being apparently much larger than it was assumed in our former work. Our present values for the function F_1^{SE} are in a marginal agreement with the result by Blundell *et al.* [12] and deviate by 1.5σ from the preliminary result by Nio [38].

The Uehling part of the vacuum-polarization hfs correction is given in the next line of Table V. The numerical values are taken from Table IV for $Z=1$ and 2 and from Refs. [6,33] for $Z=0$. The electric-loop WK correction for $Z=1$ and 2 was calculated directly in Sec. II; the corresponding numerical value for $Z=0$ was obtained by a simple extrapolation. Extrapolation was also employed in order to obtain the results for the magnetic-loop WK part of the vacuum-polarization correction presented in the table. The error bars specified are obtained under the assumption that the logarithmic contribution to the next-to-leading order enters with a coefficient of about 2.

We now turn to the experimental consequences of our calculation. As demonstrated in Ref. [6], the higher-order self-energy correction is one of the major sources of uncertainty of the theoretical prediction for the normalized difference of the hfs intervals $\Delta_{21}=8\nu_{2s}-\nu_{1s}$ for the $^3\mathrm{He}^+$ ion. Our present calculation changes the theoretical value of this correction by -0.056 kHz (as compared to our former result [14]) and improves its accuracy by a factor of 2. The resulting value of the one-loop QED contribution that incorporates all orders in $Z\alpha$ starting with the constant term to order $\alpha(Z\alpha)^3E_F$ for the $^3\mathrm{He}^+$ ion is given in the first line of Table VI. In the next lines of the table, we give the total theoretical

TABLE V. One-loop higher-order QED correction. SE denotes the self-energy contribution, Ue the Uehling part, WK-EL the electric-loop WK part, and WK-ML the magnetic-loop WK part.

	$F_1(0\alpha)$	$F_1(1\alpha)$	$F_1(2\alpha)$	$F_{21}(0\alpha)$	$F_{21}(1\alpha)$	$F_{21}(2\alpha)$	Reference
SE	−13.2(4)	−13.8(3)	−14.1(3)	8.4(5)	7.6(4)	7.2(3)	
		−12.0(2.0)					[12]
		−14.3(1.1)	−14.5(7)		6.5(8)	6.3(6)	[14]
	−15.9(1.6)						[38]
Ue	7.06	7.23	7.34	2.32	2.32	2.31	
WK-EL	−0.11	−0.12	−0.12	0.00	0.00	0.00	
WK-ML	−0.69(15)	−0.69(12)	−0.69(7)	0.00	0.00	0.00	
Total	−6.9(4)	−7.4(3)	−7.6(3)	10.7(5)	9.9(4)	9.5(3)	

TABLE VI. Normalized difference of the hfs intervals $\Delta_{21} = 8\nu_{2s} - \nu_{1s}$ for the $^3He^+$ ion, in kHz.

Higher-order QED correction	−0.594(19)	
Δ_{21}, old theory	−1 190.068(64)	(Ref. [6])
Δ_{21}, new theory	−1 190.124(55)	
Δ_{21}, experiment	−1 189.979(71)	(Refs. [2,3])

value for the difference $\Delta_{21}(^3He^+)$ taken from Ref. [6], this value modified by the present calculation, and the corresponding experimental result. As can be seen from the table, our calculation increases the deviation of the theoretical prediction from the experimental value from 0.9σ to 1.6σ.

It should be noted that our numerical results for all corrections at $Z=1$, except for the one for the magnetic-loop WK contribution, can be directly applied to the hyperfine splitting in muonium. Our calculation of the magnetic-loop WK correction does not hold for muonium since it involves a regularization by an extended magnetization distribution of the nucleus and a subtraction of the related contribution to the measured value of the nuclear magnetic moment. In the case of muonium, the nucleus is substituted by a pointlike muon and the regularization should be performed by a finite mass of the muon rather than by a finite size.

SUMMARY

In the present investigation, we carried out an all-order (in $Z\alpha$) calculation of the one-loop QED correction to the hyperfine splitting of the $1s$ and $2s$ states in light H-like ions. This calculation significantly improved the accuracy of this correction, as compared to the previous evaluations. By subtracting the known terms of the $Z\alpha$ expansion and extrapolating the remainder to lower values of Z, we obtained the results for the higher-order remainder for $Z=0$, 1, and 2. Our calculation shifts the theoretical value of the normalized difference Δ_{21} of the $1s$ and $2s$ hfs intervals in $^3He^+$ by 0.056 kHz and slightly improves its accuracy.

Note added. Recently, we learned that the result of Ref. [6] quoted in Table VI as "Δ_{21}, old theory" contained an error due to a misprint in the expression for the nuclear magnetic moment. The corrected value (which includes a more conservative than in [6] estimate of the uncertainty of the self–energy correction) is -1 190.083(150) [S. G. Karshenboim and V. G. Ivanov, e-print hep–ph/0507322]. Consequently, the entry "Δ_{21}, new theory" in Table VI becomes -1190.139(55), which deviates by 1.8σ from the experimental value.

ACKNOWLEDGMENTS

This work was supported in part by RFBR (Grant No. 04-02-17574) and by DFG. A.N.A. and V.A.Y. acknowledge support from the "Dynasty" foundation and from INTAS (Grants No. YS 03-55-960 and No. YS 03-55-1442). G.P. acknowledges financial support from BMBF and GSI.

[1] M. M. Sterheim, Phys. Rev. **130**, 211 (1963).
[2] H. A. Schluessler, E. N. Fortson, and H. G. Dehmelt, Phys. Rev. **187**, 5 (1969); Phys. Rev. A **2**, 1612 (1970).
[3] M. H. Prior and E. C. Wang, Phys. Rev. A **16**, 6 (1977).
[4] N. Kolachevsky, M. Fischer, S. G. Karshenboim, and T. W. Hänsch, Phys. Rev. Lett. **92**, 033003 (2004).
[5] N. Kolachevsky, P. Fendel, S. G. Karshenboim, and T. W. Hänsch, Phys. Rev. A **70**, 062503 (2004).
[6] S. G. Karshenboim and V. G. Ivanov, Eur. Phys. J. D **19**, 13 (2002).
[7] P. J. Mohr and B. N. Taylor, Rev. Mod. Phys. **77**, 1 (2005).
[8] H. Persson, S. M. Schneider, W. Greiner, G. Soff, and I. Lindgren, Phys. Rev. Lett. **76**, 1433 (1996).
[9] V. A. Yerokhin and V. M. Shabaev, Pis'ma Zh. Eksp. Teor. Fiz. **63**, 309 (1996) [JETP Lett. **63**, 18 (1996)].
[10] S. A. Blundell, K. T. Cheng, and J. Sapirstein, Phys. Rev. A **55**, 1857 (1997).
[11] V. A. Yerokhin, V. M. Shabaev, and A. N. Artemyev, e-print physics/9705029.
[12] S. A. Blundell, K. T. Cheng, and J. Sapirstein, Phys. Rev. Lett. **78**, 4914 (1997).
[13] P. Sunnergren, H. Persson, S. Salomonson, S. M. Schneider, I. Lindgren, and G. Soff, Phys. Rev. A **58**, 1055 (1998).
[14] V. A. Yerokhin and V. M. Shabaev, Phys. Rev. A **64**, 012506 (2001).
[15] J. Sapirstein and K. T. Cheng, Phys. Rev. A **63**, 032506 (2001).
[16] U. D. Jentschura, P. J. Mohr, and G. Soff, Phys. Rev. Lett. **82**, 53 (1999).
[17] V. M. Shabaev, M. Tomaselli, T. Kühl, A. N. Artemyev, and V. A. Yerokhin, Phys. Rev. A **56**, 252 (1997).
[18] V. M. Shabaev, M. B. Shabaeva, I. I. Tupitsyn, V. A. Yerokhin, A. N. Artemyev, T. Kühl, M. Tomaselli, and O. M. Zherebtsov, Phys. Rev. A **57**, 149 (1998); **58**, 1610 (1998).
[19] A. N. Artemyev, V. M. Shabaev, G. Plunien, G. Soff, and V. A. Yerokhin, Phys. Rev. A **63**, 062504 (2001).
[20] V. A. Yerokhin, K. Pachucki, and V. M. Shabaev, Phys. Rev. A **72**, 042502 (2005).
[21] V. M. Shabaev, Phys. Rep. **356**, 119 (2002).
[22] N. J. Snyderman, Ann. Phys. (N.Y.) **211**, 43 (1991).
[23] S. A. Blundell, Phys. Rev. A **46**, 3762 (1992).
[24] V. A. Yerokhin and V. M. Shabaev, Phys. Rev. A **60**, 800 (1999).
[25] P. J. Mohr, Ann. Phys. (N.Y.) **88**, 26 (1974).
[26] P. Indelicato and P. J. Mohr, Phys. Rev. A **46**, 172 (1992).
[27] P. Indelicato and P. J. Mohr, Phys. Rev. A **58**, 165 (1998).
[28] V. A. Yerokhin, P. Indelicato, and V. M. Shabaev, Phys. Rev. Lett. **89**, 143001 (2002).
[29] V. A. Yerokhin, P. Indelicato, and V. M. Shabaev, Phys. Rev. A **69**, 052503 (2004).
[30] T. Kinoshita and M. Nio, Phys. Rev. Lett. **72**, 3803 (1994).
[31] S. M. Schneider, W. Greiner, and G. Soff, Phys. Rev. A **50**,

118 (1994).
[32] S. G. Karshenboim, Z. Phys. D: At., Mol. Clusters **36**, 11 (1996).
[33] S. G. Karshenboim, V. G. Ivanov, and V. M. Shabaev, Zh. Eksp. Teor. Fiz. **117**, 67 (2000) [Sov. Phys. JETP **90**, 59 (2000)].
[34] A. I. Milstein and A. S. Yelkhovsky, Phys. Lett. B **233**, 11 (1989); Zh. Eksp. Teor. Fiz. **99**, 1068 (1991) [Sov. Phys. JETP **72**, 592 (1991)].
[35] A. G. Fainshtein, N. L. Manakov, and A. A. Nekipelov, J. Phys. B **24**, 559 (1991).
[36] K. Pachucki, Phys. Rev. A **54**, 1994 (1996).
[37] M. Nio and T. Kinoshita, Phys. Rev. D **55**, 7267 (1997).
[38] M. Nio, in *Quantum Electrodynamics and Physics of the Vacuum*, edited by G. Cantatore, AIP Conf. Proc. No. 564 (AIP, Melville, NY, 2001), p. 178.
[39] S. G. Karshenboim, in *The Hydrogen Atom. Precision Physics of Simple Atomic Systems*, edited by S. G. Karshenboim *et al.* (Springer, Berlin, 2001), p. 335.
[40] E.-O. Le Bigot, U. D. Jentschura, P. J. Mohr, P. Indelicato, and G. Soff, Phys. Rev. A **68**, 042101 (2003).
[41] V. G. Ivanov and S. G. Karshenboim, in *The Hydrogen Atom. Precision Physics of Simple Atomic Systems* (Ref. [39]), p. 637.